

# Geotechnical characteristics and consolidation properties of Tianjin marine clay

Huayang Lei<sup>\*1,2</sup>, Shuangxi Feng<sup>1a</sup> and Yan Jiang<sup>3b</sup>

<sup>1</sup>Department of Civil Engineering, Tianjin University, Tianjin 300072, China

<sup>2</sup>Key Laboratory of Coast Civil Structure Safety of Education Ministry, Tianjin University, Tianjin 300072, China

<sup>3</sup>Terracon Consultants, Inc., 2201 Rowland Ave., Savannah, Georgia 31404, U.S.A.

(Received March 26, 2017, Revised August 2, 2017, Accepted May 12, 2018)

**Abstract.** Tianjin, which is located on the west shore of the Bohai Sea, is part of China's Circum-Bohai-Sea Region, where very weak clay is deposited. From the 1970s to the early 21<sup>st</sup> century, Tianjin marine clay deposits have been the subject of numerous geotechnical investigations. Because of these deposits' geological complexity, great depositional thickness, high water content, large void ratio, excessive settlement, and low shear strength, the geotechnical properties of Tianjin marine clay need to be summarized and evaluated based on various in situ and laboratory tests so that Tianjin can safely and economically sustain more infrastructure in the coming decades. In this study, the properties of Tianjin marine clay, especially its consolidation properties, are summarized, evaluated and discussed. The focus is on establishing correlations between the geotechnical property indexes and mechanical parameters of Tianjin marine clay. These correlations include the correlations between the water content and the void ratio, the depth and the undrained shear strength, the liquid limit and the compression index, the tip resistance and the constrained modulus, the plasticity index and the ratio of undrained shear strength and the preconsolidation pressure. In addition, the primary consolidation properties of Tianjin marine clay, such as the intrinsic compression line (ICL), sedimentation compression line (SCL), compression index,  $C_c$ , coefficient of consolidation,  $C_v$ , and hydraulic conductivity change index,  $C_{kv}$ , are evaluated and discussed. A secondary consolidation property, i.e., the secondary compression index,  $C_{\alpha}$ , is also investigated, and the results show that the ratio of  $C_{\alpha}/C_c$  for Tianjin marine clay can be used to calculate  $C_{\alpha}$  in secondary consolidation settlement predictions.

**Keywords:** marine clay; consolidation; correlations; secondary consolidation

## 1. Introduction

The Tianjin Binhai New Area (TBNA) is located on the eastern coast of Tianjin and in the centre of the Circum-Bohai-Sea Region, as shown in Fig. 1. It has an area of approximately 2270 km<sup>2</sup> and a population of approximately 2.53 million. Since the Chinese central government proposed a policy of Beijing-Tianjin-Hebei integration, the TBNA has striven to become an ocean-oriented economic development belt and a liveable coastal town centre on Tanggu with Dagang and Hangu as the two economic wings. Moreover, as a result of the rapid economic development in Tianjin, numerous urban infrastructure projects have been built or are under construction, and an increasing number of projects will be constructed to meet the demands of population expansion and urban sprawl. For example, the construction of the central business district (CBD) in the Yujiapu zone, where many high-rise buildings

have been constructed, will establish a financial innovation base in China and become a landmark in the TBNA. The construction of the Nangang industrial zone and textile industrial park, a 200 km<sup>2</sup> area in the Nangang industrial zone, will soon be completed. In addition, the Beitang zone is planning to build internationally recognized industrial parks and tourist resorts.

However, in coastal cities, the soils are typically recent marine deposits, which have high water contents, large void ratios, high compressibility, poor permeability and low shear strength, which results in unique engineering behaviours (Ebrahimian *et al.* 2012, Lei *et al.* 2015, Sun *et al.* 2015, Park 2016, Zheng 2016). Notably, excessive and differential settlement often occurs in geotechnical structures constructed on the marine deposits. For example, the ground settling that occurred at the Kansai international airport (Mesri and Funk 2014) has reached more than 12 metres since the airport opened in 1994. A highway in Beijing-Tianjin-Tangshan continues to settle at an average rate of 0.03-0.05 mm per day, as reported by Zhang (2010), and this settling has a serious impact on highway serviceability and driving safety. Shu (2013) reported that the total settling at the intersection of Shanghai road and Hebei road in Tianjin from 1959 to 2006 was 3.25 m, and the differential settlement was over 0.94 m.

The consolidation properties of clays are an interesting topic, and many types of clays have been studied, such as

\*Corresponding author, Professor  
E-mail: [leihuayang74@163.com](mailto:leihuayang74@163.com)

<sup>a</sup>Ph.D. Student

E-mail: [shuangxiyaokaoyan@163.com](mailto:shuangxiyaokaoyan@163.com)

<sup>b</sup>Ph.D.

E-mail: [yanjiang.geo@gmail.com](mailto:yanjiang.geo@gmail.com)

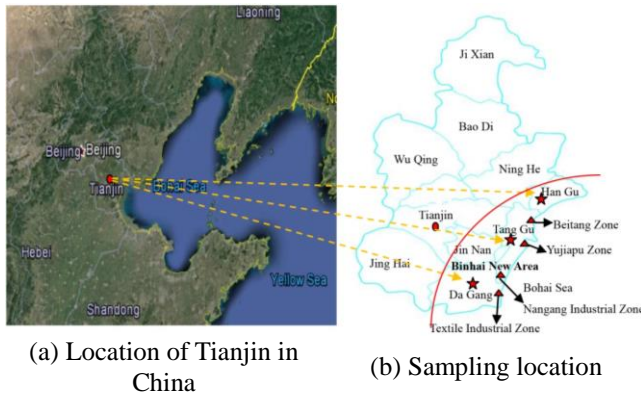


Fig. 1 Tianjin's geographic locations (adapted from Google)

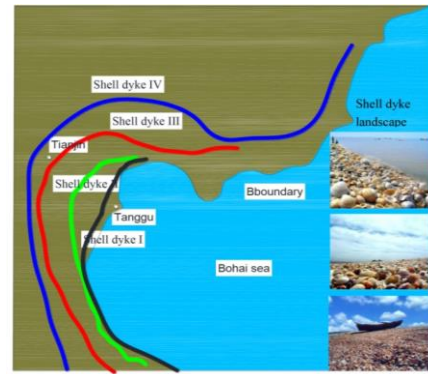


Fig. 2 Shell dyke distribution

Ariake clay, Singapore clay, London clay, Eastern Canadian clay, Lianyungang clay, and Shanghai clay (Cai *et al.* 2007, Arulrajah and Bo 2008, Du *et al.* 2008, Yin *et al.* 2009, Yang and Gong 2010, Wu *et al.* 2015). Similarly, an increasing number of experimental and theoretical studies on the consolidation properties of Tianjin marine clay can be found in Wei *et al.* (2010), Yang *et al.* (2010), Yang (2011) and Ma (2014). In addition to the primary consolidation properties, researchers have focused on secondary consolidation properties (Chen *et al.* 2014, Wu 2015), which are characterized by continuous compression subjected to constant effective stress. The secondary consolidation properties of marine clays play an important role in the long-term stability and settlement of structures built on such clays. Yang (2011) studied the microstructure and structural strength of Tianjin hydraulic fill in the process of rheology to predict long-term deformation. In addition, the dynamic creep behaviour of Tianjin marine clay has been studied (Wang 2014).

Settling is one of the main concerns in the design of infrastructure built on reclaimed lands. Continuous settling at an annual rate of 15-20 mm due to the compression of marine clay was monitored in the TBNA, and the settling undermined the performance of various infrastructures. Hence, a better understanding of the geotechnical characteristics, particularly the consolidation properties, of Tianjin marine clay is important for consolidation settlement prediction, which influences the urban planning and environmental impact studies of urban infrastructure projects in Tianjin. In this paper, the consolidation properties of Tianjin marine clay were investigated using site investigations and laboratory tests. Tianjin marine clays were reviewed in regard to their consolidation properties. The most significant findings were the establishment and evaluation of the correlations between the basic soil property indexes and the consolidation properties. The secondary consolidation behaviour of the Tianjin clays was also evaluated.

## 2. Engineering geology properties

### 2.1 Depositional history

Understanding the depositional history is prerequisite to

studying the behaviour of Tianjin marine clay. Since the Holocene, the sedimentary strata were loose deposits in the TBNA, and their genetic types and spatial distribution were controlled and influenced by the climate and paleogeographic environment. Therefore, it is of great significance to investigate the depositional history of Tianjin clay.

From the late Pleistocene to the Holocene (70.0 ka BP~10.0 ka BP), the movements of the crust were sharply uplifted with changes in the climate. Tianjin marine clay was twice affected by the tide and the regression of the sea. Therefore, the TBNA formed a coastal shallow sea environment with a water depth of 10 m to 30 m, which led to the formation of marine deposit III and marine deposit II. As the climate cooled 25.0 ka BP, the sea level continued to drop rapidly and then retreated substantially. Therefore, all the water flowed out of the Bohai Sea, which turned into a landform.

In the early Holocene (approximately 10.0 ka BP), the global sea level rose because of the warming climate, which made the coastline move westward from the continental shelf of the East China Sea. The sea was closed to the modern coastline at approximately 9 ka BP, and the coastal swamp was widely distributed in the west of the TBNA, which primarily caused the formation of carbonaceous deposits in the floodplain.

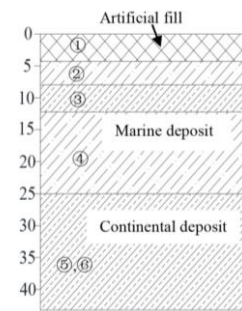
In the mid Holocene (7.5 ka BP), the TBNA sunk into the sea, forming a coastal shallow water environment with a water depth of 10 m to 30 m. At that time, marine deposit I began to form at a water depth of 30 m. Subsequently, with the climate cooling, the sea surface stopped rising at 6 ka BP. The Yellow River, carrying a variety of mud sand, flowed into the Bohai Sea from the Tianjin area. As a result, the coastline was restored, and river estuary deposition was formed. At approximately 4.0~5.0 ka BP, the diversion of the Yellow River caused the coastline to have a longer period of stability. Shell dyke IV formed with the action of the waves. In contrast, at approximately 3.8~3.0 ka BP, the crust began to rise, the Yellow River was diverted, and shell dyke III formed. In 608 BC, the Yellow River moved northward into the sea from Tianjin city, and a large amount of mud and sand was deposited in the estuary, which built the delta in a short period of time.

In the late Holocene (2.5 ka BP), the temperature decreased, the Yellow River diverted from Shandong to the

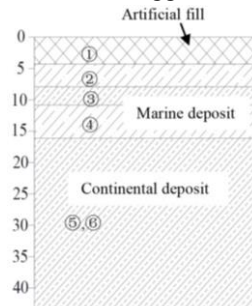
Bohai Sea, and the coastline remained in a stable state, forming shell dyke II. At 0.7~0.4 ka BP, the Yellow River moved forward to the south of China, and the coastline retreated to Tanggu, forming shell dyke I. Therefore, the shell dykes recorded and characterized the depositional history of Tianjin clays, which is shown in Fig. 2. This phenomenon reflected the changes in the land and the coastline.

Table 1 Stratigraphic distribution characteristics

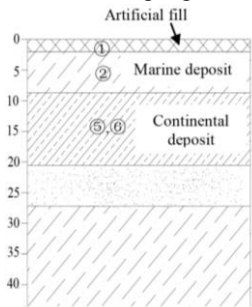
Chronologic	Geological series	Cause of formation code	Cause of formation	Stratum	Depth /m
Holocene Series	①	Q <sup>ml</sup>	Artificial fill	Artificial fill	0~4
	②		Neritic facies		4~8
	③	Q <sup>2m</sup> <sub>4</sub>	Marine-continental transitional facies	Marine deposit	6~14
	④		Neritic facies		8~25
	⑤	Q <sup>1h</sup> <sub>4</sub>	Swamp facies		10~17
	⑥	Q <sup>1al</sup> <sub>4</sub>	Floodplain deposits~ riverbed deposits	Continental deposit	12~21



(a) Tanggu



(b) Dagang



(c) Hangu

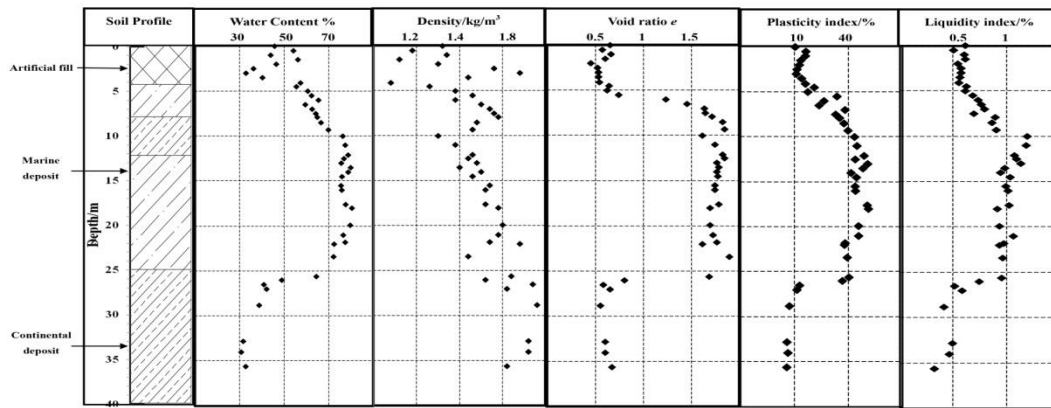
Fig. 3 Soil profiles

Table 2 Test method and test condition

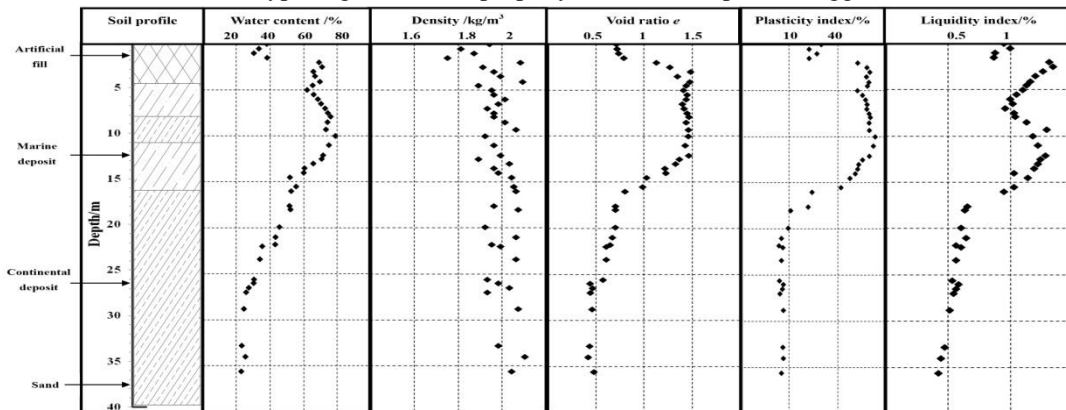
Test type/ condition	Test programme	Sample Size/mm	Test Index	Test aim
In situ tests	VST	-	Undrained shear strength	To evaluate the undrained shear strength and sensitivity of soil
	CPT	-	Cone resistance ( $q_c$ ), sleeve friction ( $f_s$ ) and pore water pressure ( $u$ )	To identify subsurface soil strata, estimate the undrained shear strength and evaluate the bearing capacity of foundation
	Liquid and Plastic limit test/Fall cone test	Diameter $\times$ Height=55 $\times$ 40	Moisture content, penetration	To provide the liquid limit and plastic limit
Macroscopic tests	Conventional oedometer tests	Diameter $\times$ Height=61.8 $\times$ 20	Coefficient of compressibility, Compression index, preconsolidation pressure, void index, coefficient of consolidation	To evaluate the consolidation behaviours of Tianjin marine clay with CH
	Laboratory tests	Triaxial tests	Diameter $\times$ Height=39.1 $\times$ 80 or 50 $\times$ 100	Constrained modulus, hydraulic conductivity, coefficient of compressibility, compression index, preconsolidation pressure, void index, coefficient of consolidation, secondary compression index
Microscopic tests	One-dimensional creep tests	Diameter $\times$ Height=61.8 $\times$ 20	Secondary compression index	To evaluate the creep characteristics of Tianjin marine clay with CH
	XRD	Area of plane=10 mm $\times$ 10 mm	Diffraction angle, diffraction strength	To determine the mineral composition
	SEM	Diameter $\times$ Height=30 $\times$ 10	Image with different magnification	Qualitatively describe the particle arrangement and pore size
	MIP	Cube=1000	Intrusion volume, pore radius	To illustrate the pore size distribution

2.2 Subsurface conditions

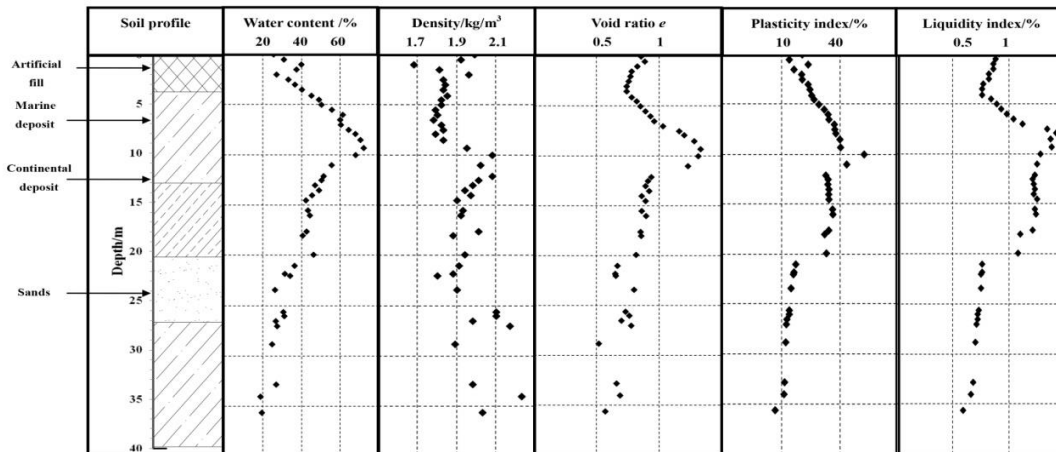
Tianjin marine clay is affected by the tide and the



(a) Typical geotechnical property index with depth at Tanggu



(b) Typical geotechnical property index with depth at Dagang



(c) Typical geotechnical property index with depth at Hangu

Fig. 4 Typical geotechnical property index with depth

regression of the sea during the Quaternary period, which affected the sea-land interactions of the sediments. According to the local design code of the Technical Specification for the Division of Subsoil Sequence in Tianjin (DB/T29-191-2009), the soil profile in the TBNA generally consists of a top layer of artificial fill followed by a layer of marine deposit and a continental deposit layer, which is the bearing stratum and primarily concentrated 10 m below. The thickness of the marine layer varies from approximately 5 m to 20 m. This Quaternary marine-

continental interlayer soil profile is typical in the TBNA and exists approximately 40 m below the ground's surface. Fig. 3 illustrates the soil profiles in Tanggu, Dagang, and Hangu in the TBNA. The characteristics of the stratigraphic distribution are shown in Table 1.

### 2.3 Soil samples

To explain the consolidation properties, the property indexes of Tianjin marine clay were obtained from 50

geotechnical investigation reports that included 1020 index tests in the TBNA. The 50 geotechnical investigation reports consist of deep foundation, tunnel, and airport projects in Tianjin. Soil samples obtained for experimental analysis can be divided into three primary categories: disturbed soil, undisturbed soil and reconstituted soil. Disturbed samples are obtained by split-barrel sampling, which will destroy the macro structure of soil but does not alter the mineralogical composition. Specimens from those samples can be used to determine the appropriate laboratory tests, for example, the water content, the liquid plastic limit, and the soil chemical tests. Conversely, undisturbed samples are obtained in clay soil strata for use in laboratory testing to determine the engineering properties of these soils (Mayne *et al.* 2001). Undisturbed samples were obtained using Shelby tubes with a tube length of 50 cm, a thickness of 0.2 cm, an internal diameter of 9.8 cm and a 6-degree tapered end. This designed aimed to minimize the disturbance to the in situ structure. Undisturbed samples can be used to determine the strength, soil preconsolidation pressure, soil structural property, and dynamic properties. In contrast, reconstituted samples are obtained using the compaction method in the laboratory according to the local code "Specification of soil test". Reconstituted samples can be used to study on the liquid limit (LL) and the plastic limit (PL) in laboratory tests.

## 2.4 Test programme

Within the 50 geotechnical investigation reports, 1020 index tests were included, and the geotechnical investigations can be divided into two types of tests: macroscopic tests and microscopic tests. Furthermore, macroscopic tests can be further divided into in situ investigations and laboratory tests. In situ investigations primarily included the vane shear test (VST) and the cone penetration test (CPT). VST is generally used to obtain the undrained strength. The CPT provides continuous measurements of the cone resistance ( $q_c$ ), sleeve friction ( $f_s$ ) and pore water pressure ( $u$ ). These measurements can be used to identify the subsurface soil strata and to estimate the geotechnical parameters, e.g., the undrained shear strength. In contrast, laboratory tests primarily include conventional oedometer tests, one-dimensional creep tests and triaxial tests in this paper. Conventional oedometer tests were carried out to characterize the compression behaviours due to consolidation. The hydraulic conductivity can be determined from the triaxial tests. One-dimensional creep tests and triaxial test were carried out on the intact specimens to characterize their creep behaviours.

In addition, microscopic X-ray diffraction (SRD) tests, scanning electron microscopy (SEM) and mercury intrusion porosimetry (MIP) were conducted. SRD was used to illustrate the mineral composition of the soil. SEM and MIP were conducted to research the pore size distribution curves and to describe the skeleton of Tianjin marine clay with CH. The test table is summarized for reader's understanding and is shown in Table 2.

## 2.5 Soil property

The mineralogy of Tianjin marine clay at different

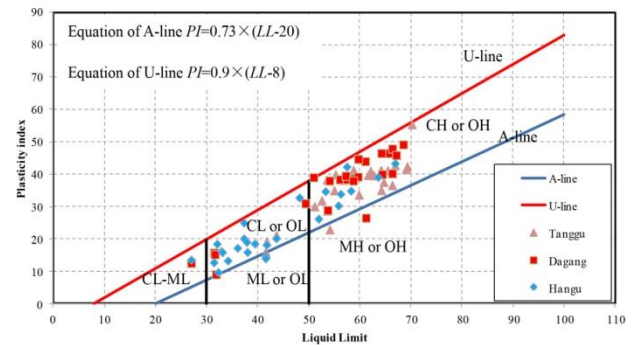


Fig. 5 Plasticity chart

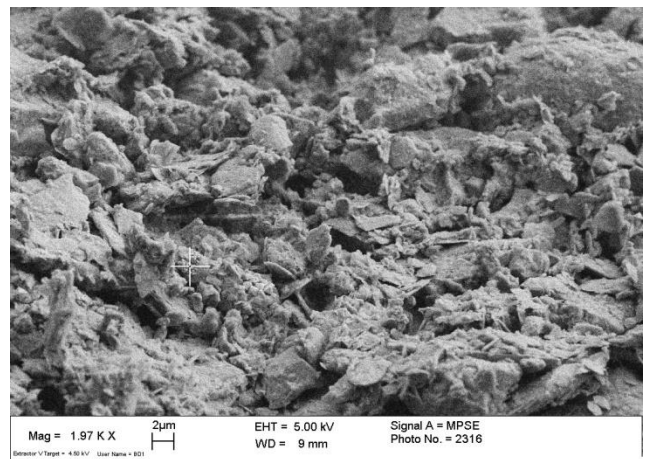


Fig. 6 Typical SEM image

depths, from 5 m to 25 m, was investigated by Du *et al.* (2010) using SRD, and their results were consistent with those from a study conducted by Wang *et al.* (2007). The clay mineralogy is consistent for the depth investigated and primarily consists of illite and montmorillonite with a small proportion of kaolinite.

The property indexes of Tianjin marine clay along the depth are shown in Figs. 4(a), 4(b), and 4(c) for the Tanggu, Dagang, and Hangu sites, respectively. The natural water content decreases with depth, from 75.9% below the artificial fill soil layer to 31.3% at 25 m. The ranges in the values of the void ratio, liquidity limit, and plasticity index are approximately 0.623-1.705, 31.7%-70.2%, and 15.1-50.2, respectively. The void ratio, liquidity limit, and plasticity index of the Tianjin marine clay in Hangu are lower than those of the clay distributed from 5 m to 25 m in Tanggu, and the values of the clay are centred at 5 m to 15 m in Dagang and 7 m to 20 m in Hangu.

Fig. 5 shows the plasticity chart for the Tianjin marine deposit. Clearly, the data points lie between the A-line and the U-line with liquid limits greater than 50%. According to the Unified Soil Classification System (USCS), most of the samples from the Tianjin marine deposit are low plasticity clays and high plasticity clays (CL-CH), which are denoted Tianjin marine clay.

## 2.6 Microfabric

The microfabric of Tianjin marine clay with CH was

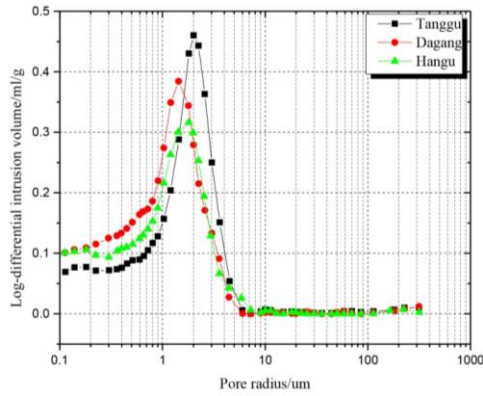


Fig. 7 Pore size distribution curves

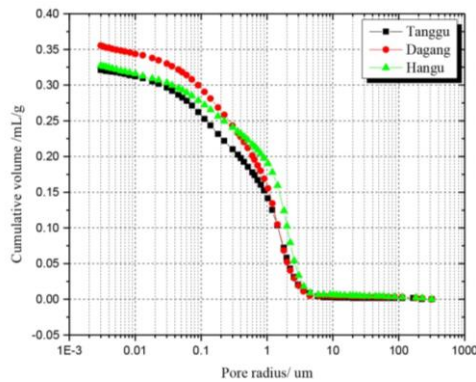


Fig. 8 Cumulative pore distribution curves

investigated using mercury intrusion porosimetry (MIP) and scanning electron microscopy (SEM). A series of test specimens were prepared from the intact soil. This paper selected a relatively typical SEM image of Tianjin marine clay, as shown in Fig. 6. Fig. 6 shows that Tianjin marine clay has single platy particles and aggregates (Jiang *et al.* 2014). The structural unit performers, including needle-like and flake soil particles with diameters less than 0.005 mm, have negatively charged surfaces. Consequently, during the particle polymerization process, most of these units must be in contact with each other along the surface-edge or surface-surface interfaces, and this contact determines the flocculated structure. Other small particles are packaged outside of the larger particles or comprise cement filling in the basic skeleton of the soil.

A series of mercury intrusion tests were conducted, and three types of relatively typical pore size distribution curves and cumulative pore distribution curves are shown in this paper. Fig. 7 presents the results of the mercury intrusion tests, which is a plot of the volume of the mercury that intruded into the pores versus the pore radius. The volume of the mercury intruded into the pores represents the volume of the pores. As shown in Fig. 7, the pore radii of the Tianjin marine clay in the Tanggu, Dagang, and Hangu areas fall within 0.1  $\mu\text{m}$  to 6  $\mu\text{m}$ . The volume of the pores increases with the pore radius and reaches a maximum when the pore radius approaches 2  $\mu\text{m}$ . Then, the volume of the pore rapidly decreases to zero when the pore radius is close to 6  $\mu\text{m}$ . Overall, the distribution of the pore volume versus the pore radius for the Tianjin marine clay was

similar in the three areas. The peak diameter can exceed 1  $\mu\text{m}$ , which demonstrates that Tianjin marine clay has large void ratios.

Jiang *et al.* (2014) divided the pore size of the soil into four types based on the pore radius, and the types are large pores, medium pores, small pores, and micropores. Large pores have a radius,  $r$ ,  $> 2 \mu\text{m}$ , medium pores have a radius  $0.2 \mu\text{m} < r < 2 \mu\text{m}$ , small pores have a radius  $0.02 \mu\text{m} < r < 0.2 \mu\text{m}$ , and micropores have a radius  $r < 0.02 \mu\text{m}$ . Fig. 8 shows that Tianjin marine clay is dominated by large and medium size pores, which account for approximately 65% of the total pore volume. The statistical analysis revealed that pores with a radius exceeding 2  $\mu\text{m}$  account for approximately 46% of the pores. In contrast, pores with radius exceeding 0.2  $\mu\text{m}$  (i.e., micropores) comprise approximately 66%. This soil has a weak cohesive force, and the reunion phenomenon is difficult to achieve. These results explain why Tianjin marine clay exhibits a flocculated structure.

## 2.7 Undrained shear strength and constrained modulus

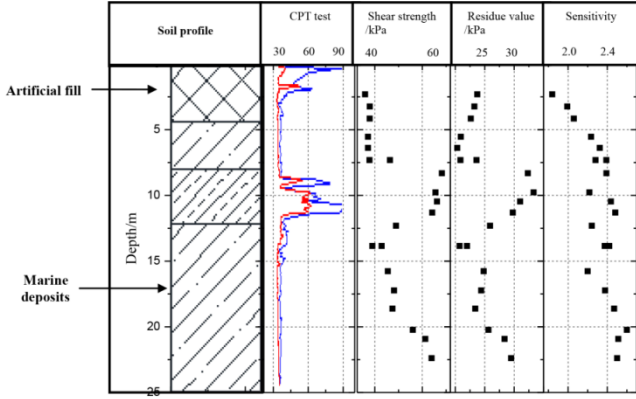
The undrained shear strength and constrained modulus are two important mechanical parameters used to evaluate the engineering behaviour of the clay. In situ tests, such as cone penetration tests (CPTs) and vane shear tests (VSTs), were performed in the Tanggu, Dagang, and Hangu areas. Fig. 9 shows that the tip resistance,  $q_c$ , and the sleeve-frictional resistance,  $f_c$ , from the CPTs, the undrained shear strength,  $C_u$ , the residual strength,  $C_u'$ , and the sensitivity,  $S_t$ , from the VSTs varied with the depth in the Tanggu, Dagang, and Hangu areas, where  $S_t$  can be defined as the ratio between  $C_u$  and  $C_u'$  (Das and Sobhan 2013). The undrained shear strength of the Tianjin marine clay measured with the field vane linearly increases with depth from 23.3 kPa at 9.3 m to 61.17 kPa at 20 m. The average sensitivity,  $S_t$ , was approximately 2.43.

Empirical correlations have been used to estimate the advanced soil parameters from the complex or time-consuming tests using the property indexes, which can be easily obtained from laboratory or in situ tests. This section summarizes several correlations used to estimate the strength and modulus for Tianjin marine clay. To clearly understand the correlations among the data, regression equations were obtained by curve fitting, and the number of data points,  $n$ , the correlation coefficient,  $R^2$ , and the standard error of the dependent variable,  $S.E.$ , are presented to illustrate the potential biases, which is convenient for engineers and is applied in engineering practice.

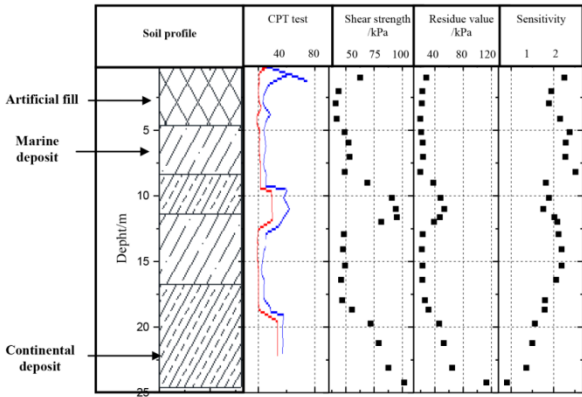
The undrained shear strength,  $C_u$ , is plotted versus the depth of the Tianjin marine clay in Fig. 10. Fig. 10 demonstrates that the undrained shear strength of the Tianjin clay correlates with the depth according to the following relationship

$$C_u = 3.53H - 9.46 \quad (1)$$

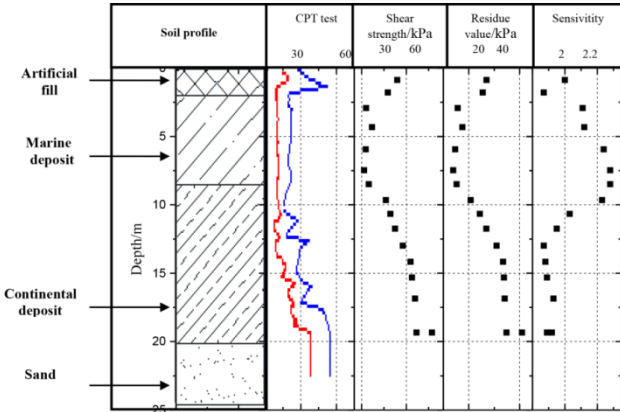
The undrained shear strength,  $C_u$ , is normalized with respect to the preconsolidation pressure,  $p_c$ , which is measured via a conventional one-dimensional test. The



(a) CPT and VST indexes measured at Tanggu

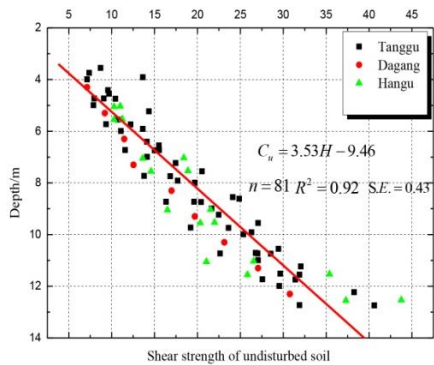


(b) CPT and VST indexes measured at Dagang



(c) CPT and VST indexes measured at Hangu

Fig. 9 Typical geotechnical property indexes: CPT and VST



(Note:  $n$ =number of data;  $R^2$ =correlation coefficient;  $S.E.$ =standard error of dependent variable)

Fig. 10 Correlation between the undrained shear strength and depth

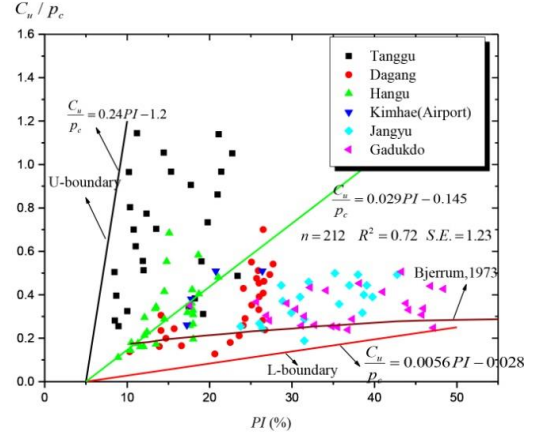


Fig. 11 Correlation between  $C_u/p_c$  and  $PI$

normalized undrained shear strength,  $C_u/p_c$ , is correlated with the plasticity index,  $PI$ , for Tanggu, Dagang and Hangu, as shown in Fig. 11.

$$\frac{C_u}{p_c} = 0.029PI - 0.145 \quad (2)$$

The data from Jangyu, Kimhae and Gadukdo (Chung *et al.* 2002) and the results of Bjerrum (1973) are summed in Fig. 11. Undoubtedly, the data from Tanggu, Dagang, and Hangu are discrete, and the  $S.E.$  exceeds 1.0. However, the data fall with range of the U-boundary and the L-boundary, which can be applied to predict the minimum value, the mean value and the maximum value of  $C_u$  for engineers. The U-boundary and the L-boundary are determined by a confidence interval that is 95% of variance according to the results of Xia *et al.* (2008).

The different correlations between  $C_u/p_c$  and  $PI$  compared with others are attributed to different indexes of  $PI$  corresponding to the different rotation angles with respect to the vane test.

The vane strength is derived from shearing in the top and bottom horizontal planes and from horizontally shearing of the vertical cylindrical surface. Based on the assumption that the shear stress distribution is uniform on the vertical and the horizontal surfaces, the torque required to turn the vane is given in Eq. (3)

$$T = \frac{\pi D^2 H \tau_v}{2} + \frac{\pi D^3 \tau_h}{6} \quad (3)$$

where  $D$  and  $H$  are the diameter and height of the vane, and  $\tau_v$  and  $\tau_h$  are the shear stresses on the vertical and horizontal planes, respectively. For  $H=2D$  and  $\tau_v = \tau_h = C_u$ , the undrained shear strength is computed from the measured peak torque using Eq. (4)

$$C_u = \frac{6T}{7\pi D^3} \quad (4)$$

According to the results reported by Bjerrum (1973), different indexes of  $PI$  correspond to different rotation angles, and in Eq. (4),  $T$  is related to the rotation angle.

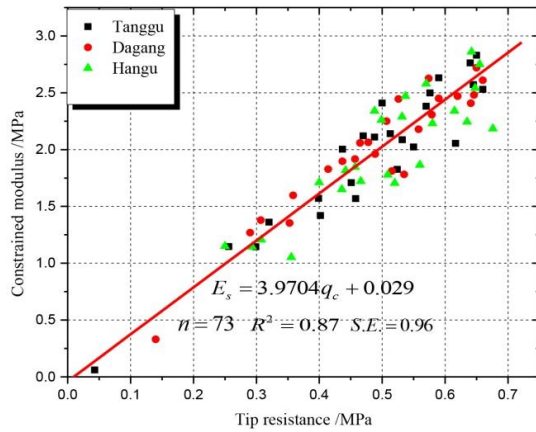


Fig. 12 Correlation between the tip resistance and constrained modulus

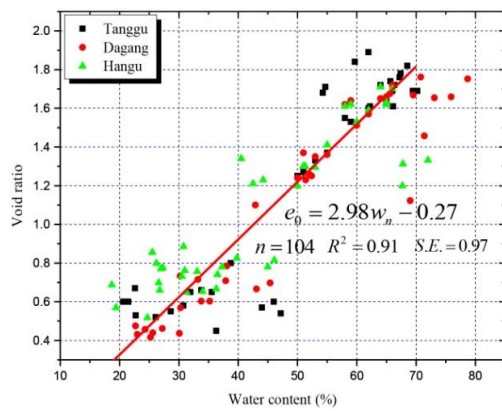


Fig. 13 Water content versus void ratio

Therefore,  $C_u$  is directly affected by  $PI$ . Because different indexes of  $PI$  are presented in different regions, a unique correlation between  $C_u/P_c$  and  $PI$  is present in the TBNA. When  $0.2 \text{ MPa} < q_c < 0.7 \text{ MPa}$ , a correlation between the tip resistance,  $q_c$ , and the constrained modulus,  $E_s$ , can be represented as follows (Fig. 12)

$$E_s = 3.9704q_c + 0.029 \quad (5)$$

Fig. 13 shows the data points used for the correlation between  $w_n$  and  $e_0$ . The correlation is expressed in Eq. (6)

$$e_0 = 2.98w_n - 0.27 \quad (6)$$

As for saturated soil, the void ratio is related to the values of the water content and the specific gravity. Eq. (4) can be used to evaluate the specific gravity and the void ratio for a given water content, which makes it convenient for engineers to make an appropriate decision.

### 3. Consolidation properties of Tianjin marine clay

#### 3.1 Compression index

Conventional oedometer tests were performed on Tianjin marine clay to characterize the compression

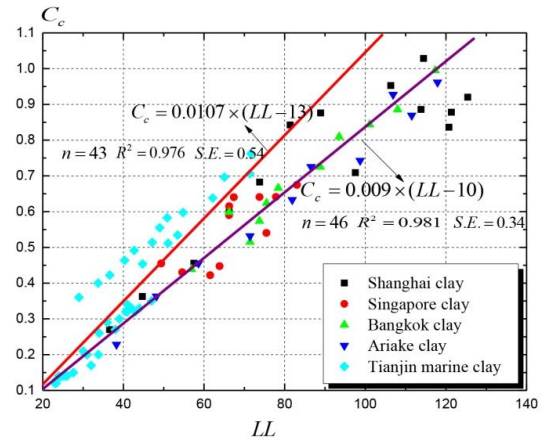


Fig. 14  $C_c$  versus  $LL$

Table 3 Correlations between  $C_c$  and  $LL$

Nation	Area	Empirical Equation	Reference
China	Tianjin	$C_c = 0.0107(LL - 13)$	Jiang <i>et al.</i> (2014)
	Shanghai	$C_c = 0.009(LL - 10)$	
	Dalian	$C_c = 0.009(LL - 10)$	
Thailand	Bangkok	$C_c = 0.008(LL + 0.21)$	Brand <i>et al.</i> (1981)
France	Gard	$C_c = 0.0147 LL - 0.213$	Brand <i>et al.</i> (1981)
Greece	Athens	$C_c = 0.006(LL - 9)$	Brand <i>et al.</i> (1981)
Singapore	Singapore city	$C_c = 0.009(LL - 10)$	Tanaka <i>et al.</i> (2001)
Brazil	Teresina	$C_c = 0.0046(LL - 9)$	Brand <i>et al.</i> (1981)
Japan	Ariake	$C_c = 0.009(LL - 10)$	Jiang <i>et al.</i> (2014)

behaviours due to consolidation. The compression index,  $C_c$ , is a key parameter that represents the compressibility of the clay. The  $C_c$  values of Tianjin marine clay were obtained from one-dimensional consolidation tests. Overall, the  $C_c$  value of Tianjin marine clay ranged from 0.1 to 1.0. The  $C_c$  values in Tanggu were greater than those in Dagang and Hangu. In engineering practice, it is more convenient to obtain  $C_c$  using a correlation between  $C_c$  and the basic soil properties, such as the liquid limit, natural water content, and void ratio, which can be easily obtained from simple laboratory tests. This section establishes a correlation between  $C_c$  and the liquid limit,  $LL$ , for Tianjin marine clay. Fig. 14 shows a plot of  $C_c$  versus  $LL$ , and Eq. (7) expresses a linear correlation between  $C_c$  and  $LL$ .

$$C_c = 0.0107(LL - 13) \quad (7)$$

For the purpose of comparison, the correlation between  $C_c$  and  $LL$  for clays from Shanghai, Singapore, and Bangkok is also shown in Fig. 14 and Table 3 (Jiang *et al.* 2014). Fig. 14 shows that the  $C_c$  of Tianjin marine clay is larger than that in other areas with the same  $LL$ , and the  $C_c$

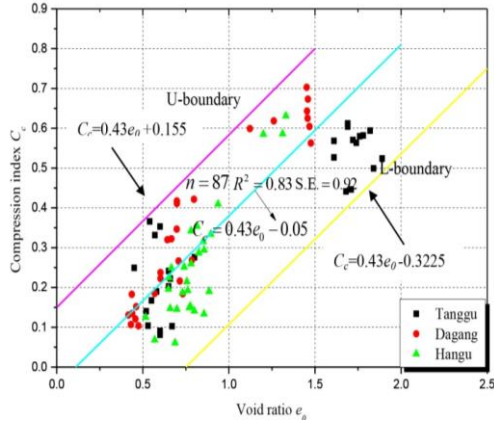
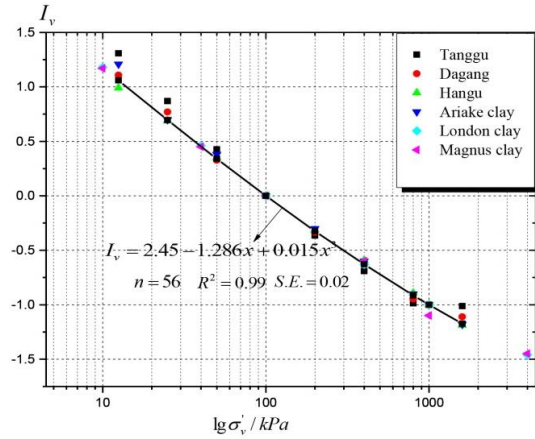

 Fig. 15  $C_c$  versus  $e_0$ 


Fig. 16 Intrinsic compression line (ICL)

 Table 4 Correlations between  $C_c$  and  $e_0$ 

Nation	Region of applicability	Empirical Equation	Reference
China	Tianjin marine clay	$C_c = 0.43e_0 - 0.05$	
	Lianyungang	$C_c = -0.63 + 0.78e_0$	
	Shanghai	$C_c = 0.589(e_0 - 0.575)$	Wei <i>et al.</i> (1980)
America	Chicago clays	$C_c = 0.208e_0 + 0.0083$	Das and Sobhan (2013)
	southern coastal clay	$C_c = 0.54(e_0 - 0.3)$	Yoon <i>et al.</i> (2011)
Korea	eastern coastal clay	$C_c = 0.39(e_0 - 0.13)$	Yoon <i>et al.</i> (2011)
	western coastal clay	$C_c = 0.37(e_0 - 0.28)$	Yoon <i>et al.</i> (2011)

increases with an increase in the  $LL$ . When the  $LL$  reaches 95,  $C_c$  may be greater than 1.0. Additional correlations between  $C_c$  and  $LL$  are tabulated in Table 3. Table 3 shows that the slope of the straight line in Tianjin is greater than the slope in other regions, except for Athens, Greece, which means that Tianjin marine clay has higher compressibility.

In addition to the correlation between  $C_c$  and  $LL$ , another correlation between  $C_c$  and the void ratio,  $e_0$ , was established because  $e_0$  influences the compressibility. This correlation is useful for engineers to estimate the  $C_c$  of Tianjin marine clay when  $e_0$  is available. Fig. 15 shows a plot of  $C_c$  versus  $e_0$ , and Eq. (8) expresses the correlation between  $C_c$  and  $e_0$

$$C_c = 0.43e_0 - 0.05 \quad (8)$$

The correlations between  $C_c$  and  $e_0$  for the clays in other areas are summarized in Table 4. These results indicated that the correlation describing the  $C_c$  of Tianjin marine clay is different from that built for the clays in other typical soft soil areas (Das and Sobhan 2013, Wu *et al.* 2015). For example,  $C_c$  is 0.22 and 0.34 for the Chicago clay and the eastern coastal clay in Korea when  $e_0$  is assumed to be 1; furthermore,  $C_c$  is 0.38 for Tianjin marine clay, which is approximately 73% and 12% greater than that of Chicago clay and eastern coastal clay in Korea. This comparison indicates that Tianjin marine clay has relatively high compressibility.

### 3.2 Intrinsic compression line (ICL) and sedimentation compression line (SCL)

Evaluating the effects of the soil structure on the mechanical behaviour of natural sedimentary soils is important in explaining the engineering behaviour of soils. Burland (1990) introduced a void index,  $I_v$ , to normalize the compression curves of various reconstituted clays at liquid limits ranging from 25% to 160% and proposed the ICL to evaluate the in situ compressive behaviour of natural sedimentary soils. The void index is defined as follows

$$I_v = \frac{e - e_{100}^*}{e_{100}^* - e_{1000}^*} = \frac{e - e_{100}^*}{C_c^*} \quad (9)$$

where  $e_{100}^*$  and  $e_{1000}^*$  are the void ratios of the reconstituted clays at effective vertical stresses of 100 kPa and 1000 kPa, respectively, and  $C_c^*$  is the intrinsic compression index. Using  $I_v$ , Burland (1990) normalized the compression curve as the ICL, which is expressed as the following

$$I_v = 2.45 - 1.286x + 0.015x^3 \quad (10)$$

where  $x$  is  $\lg \sigma'v$ , and  $\sigma'v$  is the effective consolidation pressure.

The relationship between the void index,  $I_v$ , and the effective stress,  $\sigma'v$ , for the reconstituted Tianjin marine clay was compared with the ICL proposed by Burland in Fig. 16. This comparison revealed that the ICLs for the reconstituted Tianjin marine clay, Ariake clay, London clay and Magnus clay (Hong and Takashi 1999, Hong *et al.* 2004) were consistent with the ICL proposed by Burland.

Fig. 16 can be used to determine the compactness or looseness of marine clay. According to Burland's research results, when the void index,  $I_v$ , is less than zero, the sediment is dense, and when the void index,  $I_v$ , is greater than zero, the sediment is loose. When  $\lg \sigma'v$  is approximately 100 kPa, the void index,  $I_v$ , is close to zero. The void ratio of Tianjin marine clay may be related to the soil stress history and depositional condition. In geotechnical engineering, consolidation tests are time consuming, but the ICL provides a new reference guide for engineers to evaluate the compressibility of Tianjin marine clay using oedometer testing of reconstituted clays.

As all natural clays have reached their present state due to the combined effects of the deposition environment,

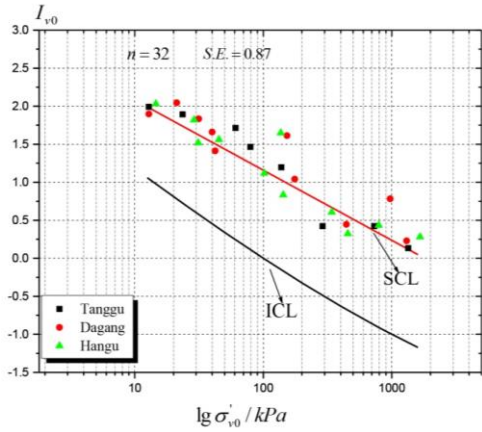


Fig. 17 Sedimentation compression line (SCL)

elapsed time, and stress history, it is likely that they have natural characteristics that are different from the intrinsic characteristics. Burland (1990) proposed the SCL, which is expressed in terms of the void index,  $I_{v0}$ , versus the effective overburden pressure,  $\sigma'_{v0}$ , where  $I_{v0}$  is similar to  $I_v$  and is defined as follows

$$I_{v0} = \frac{e_0 - e_{100}^*}{e_{100}^* - e_{1000}^*} \quad (11)$$

where  $e_0$  represents the in situ void ratio or initial void ratio. The relationship between  $I_{v0}$  and  $\lg \sigma'_{v0}$  was investigated to be used as a reference for evaluating the structural degree of natural clays. The data were obtained from Tanggu, Dagang and Hangu at depths of 7 m to 12 m in a borehole. Fig. 17 shows the data ( $I_{v0}$ ,  $\lg \sigma'_{v0}$ ) plotted from the 3 considered sites. The SCL is above the ICL, and the SCL will converge towards the ICL as  $\sigma'_{v0}$  increases. The data are close to or above the SCL, which indicates that the clays have certain structural characteristics.

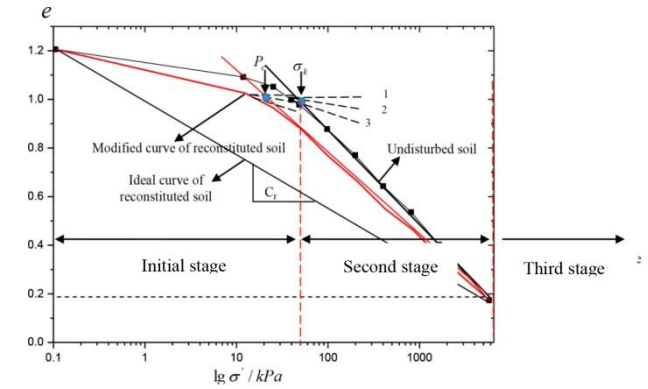
### 3.3 Preconsolidation pressure

The preconsolidation pressure is a parameter that reflects the past maximum effective stress that the soil encountered in its geological history. The preconsolidation pressure is also important for settlement prediction. Cassagrande (1932) proposed an empirical graphical method to determine the preconsolidation pressure. To determine the preconsolidation pressure of structural soft soil, the paper adopted Wang *et al.* (2007) study, which stated that the structural yield stress refers to the stress of the undisturbed soil during the compression process when the soil structure and intergranular connection begin to break.

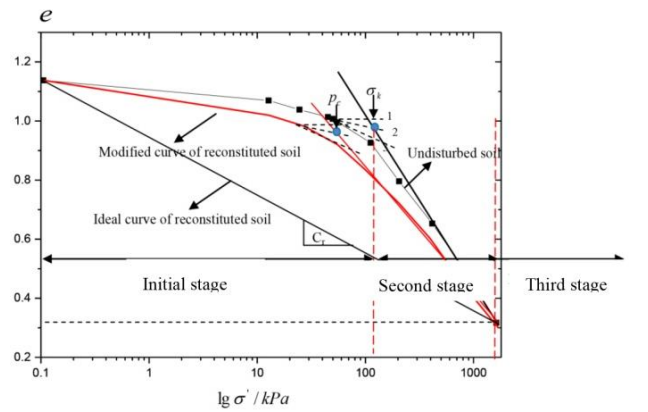
To investigate the preconsolidation pressure and structural strength of Tianjin marine clay, both undisturbed soil and reconstituted soil are prepared for the one-dimensional consolidation tests. For the reduction of sampling disturbance, Shelby tubes are used to take soil samples at Tanggu, Dagang and Hangu at depths of 10.5 m to 12 m. The tube length is 50 cm, and the thickness is 0.2 cm, with an internal diameter of 9.8 cm and 6 degrees tapered end.

Table 5 Parameter values for the modified curve of the reconstituted soil

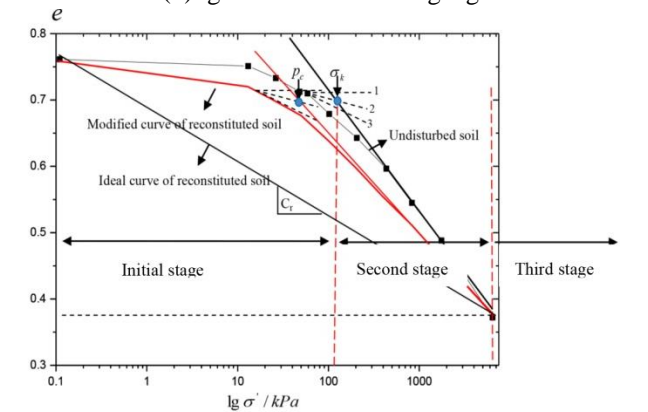
Location	$e_0$	$C_r$	$P_l$	$C_s$	A	Relationships
Tanggu	1.21	0.15	5000	0.03	2.94	$e = 1.21 - 0.0118(\lg p)^{2.94}$
Dagang	1.13	0.044	1230	0.03	1.93	$e = 1.13 - 0.0154(\lg p)^{1.93}$
Hangu	0.76	0.053	6500	0.03	1.91	$e = 0.76 - 0.0158(\lg p)^{1.91}$



(a)  $\lg \sigma'$  vs.  $e$  curve at Tanggu



(b)  $\lg \sigma'$  vs.  $e$  curve at Dagang



(c)  $\lg \sigma'$  vs.  $e$  Curve at Hangu

Fig. 18  $\lg \sigma'$  versus  $e$  Curves

The study used the ideal curve of the reconstituted soil to determine the parameter  $C_r$  and used the modified curve of the reconstituted soil to determine the preconsolidation

pressure,  $P_c$ . The yield stress,  $\sigma_k$ , was determined using a compression curve of the undisturbed soil. Usually, the difference between the structural yield stress of the undisturbed soil and the preconsolidation pressure is known as the structural strength of the soil (Du *et al.* 2010). A modified curve of the reconstituted soil can be determined using Eq. (12) and Eq. (13) as follows

$$e = e_0 - C_r (\lg p_l)^{1-A} \bullet (\lg p)^A \quad (12)$$

$$A = 1 + \frac{\lg\left(\frac{C_s}{C_r}\right)}{\lg\frac{\lg\sigma_k}{\lg p_l}} \quad (13)$$

where  $e_0$  is the initial void ratio,  $C_r$  is the slope of the ideal curve of the reconstituted soil,  $P_l$  is the pressure value corresponding to the intersection point between the reconstructed sample and the original sample compression curve, and  $C_s$  is the swelling index. According to research results from Yang (2011), the empirical value of  $C_s$  is approximately 0.03. The parameter values for the modified curve of the reconstituted soil are listed in Table 5.

Fig. 18 shows the preconsolidation pressures of the marine clays at Tanggu, Dagang, Hangu, which are 18 kPa, 58 kPa, and 64 kPa, respectively. The structural yield stresses of the Tianjin marine clays are 41 kPa, 112 kPa, and 108 kPa, respectively. Therefore, the structural strength values for the Tianjin marine clays at Tanggu, Dagang, and Hangu are 23 kPa, 54 kPa, and 44 kPa, respectively.

Most Tianjin marine clay can be described by three stages: the initial stage, the second stage, and the third stage. When the pressure is lower than the structural yield stress, i.e.,  $p < \sigma_k$ , the curve is relatively smooth and flat in the initial stage. Although some of the soil structure is damaged, the soil is undergoing elastic deformation under the limit of its structural strength. When the pressure exceeds the yield stress, i.e.,  $p > \sigma_k$ , most of the soil structure is damaged, and the compression curve tends to be steep fall in the second stage. At that moment, soil particles will slip, and soil pores will collapse. As the load gradually increases, the structure of the soil will vanish in the third stage, and the property of undisturbed soil is same as that of reconstituted soil.

The structural strength and structural behaviour of the clays are inherent because the material's connection strength develops via the process of deposition. Tianjin marine clay shows this structural strength. The factors that affect the structural strength of Tianjin marine clay include the mineral composition, the stress history of the soil and the drainage conditions during consolidation. When the stress level is low, the clay shows good mechanical properties. When the stress is too high, the structure is destroyed, which leads to large deformation.

The structural properties of the reconstituted soil are poor because of the weak structure. Tianjin marine clay and reconstituted clay with the same moisture content were examined in this paper. A consolidation test was conducted, and the structural strength values of Tianjin marine clay are

Table 6 Structural strength of Tianjin marine clay

Type of Tianjin marine clay	Structural yield stress of Undisturbed soil (kPa)	Preconsolidation pressure of reconstituted soil (kPa)	Structural strength (kPa)
Tianjin marine clay	41 - 130	18 - 62.8	23 - 67.2

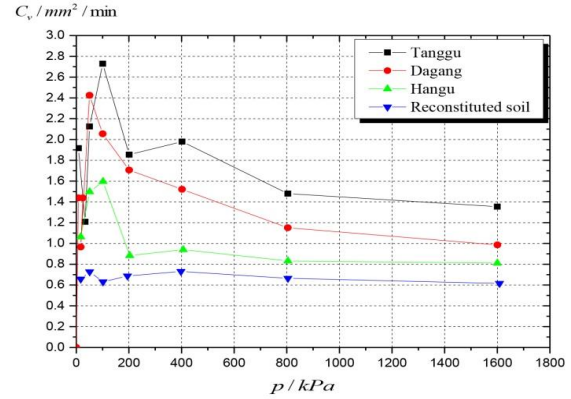


Fig. 19  $C_v$  versus  $p$  Curves

summarized in Table 6 (Wu 2015). Structural strength values ranging from approximately 23 kPa to 67.2 kPa were found for Tianjin marine clay.

### 3.4 Coefficient of consolidation

The coefficient of consolidation,  $C_v$ , is an important parameter for consolidation rate prediction. Therefore, an accurate estimation of  $C_v$  is important to predict the rate of consolidation. Calculating  $C_v$  requires a consolidation curve with an obvious boundary between the primary consolidation and secondary consolidation, according to the theory underlying the time-logarithm method. The coefficient of consolidation is calculated using Eq. (14) according to a local code "specification of soil test" (SL237-1999) (Ministry of Water Resources of the People's Republic of China 1999)

$$C_v = \frac{0.198}{t_{50}} H^2 \quad (14)$$

where  $t_{50}$  is the time for the consolidation rate to reach 50%,  $H$  is the height of the sample.

To ensure the high quality of the samples (Wang and Wei 1994), Shelby tubes are used to obtain soil samples in Tanggu, Dagang and Hangu at depths of 9.2 m to 12.4 m. Fig. 19 shows the variation in the calculated  $C_v$  for Tianjin marine clay based on the time-logarithm method at different pressures. Overall, the calculated  $C_v$  is in the range between  $0.1 \times 10^{-3}$  and  $0.5 \times 10^{-3}$  ( $\text{cm}^2/\text{s}$ ). As shown in Fig. 19, the calculated coefficient of consolidation rapidly increased and reached the maximum value at consolidation pressures of approximately 150 kPa. Subsequently, the calculated  $C_v$  gradually decreased to a stable value. Terzaghi's one-dimensional consolidation theory (Terzaghi 1925) assumes that  $C_v$  remains constant during the consolidation. However, this assumption leads to a large deviation in the consolidation rate prediction if the variation in  $C_v$  with the

consolidation pressure is ignored (shown in Fig. 19). Therefore, a reasonable estimation of  $C_v$  that considers the variation in the consolidation pressure range during consolidation is necessary for the consolidation rate prediction.

When the consolidation pressure,  $p$ , is less than the structural strength of the yield stress,  $\sigma_k$ , of 41 kPa for the Tanggu sample, the coefficient of consolidation will increase gradually. Because the pore is compressed but does not collapse, the drainage channels are not blocked. This means the drainage is fast, and the coefficient of consolidation increases. When the consolidation pressure,  $p$ , exceeds 41 kPa, the coefficient of consolidation decreases. When  $p$  is 800 kPa, the curve tends to be stable. This finding can be attributed to pore collapse, which can lead to blocked drainage channels. As a result, the drainage performance gradually decreases, and the coefficient of consolidation decreases. As the consolidation pressure increases, the coefficient of consolidation,  $C_v$ , is approximately 1.4 mm<sup>2</sup>/min, and the soil eventually behaves like reconstituted soil. The engineering properties of the Tianjin marine clays at Dagang and Hangu are similar to those of the Tianjin marine clay at Tanggu. The structural strengths of the yield stress at Dagang and Hangu are 112 kPa and 108 kPa, respectively. For the reconstituted soil, the variation in the amplitude of  $C_v$  is approximately 0-0.8 mm<sup>2</sup>/min under the various consolidation pressures. As the consolidation pressure increases, the coefficient of consolidation is approximately 0.7, which is less (by approximately 1/3-1/2) than that of the undisturbed soil.

### 3.5 Overconsolidation ratio

The overconsolidation ratio (OCR) is an important parameter to evaluate the deformation and strength characteristics of Tianjin marine clay. This section aims to investigate the changes in the OCR with depth and the difference between the OCR obtained by VST and the OCR determined by conventional oedometer tests.

The OCR is defined by

$$OCR = \frac{p_c}{\sigma'} \quad (15)$$

where  $\sigma'$  is the effective stress,  $p_c$  is the preconsolidation pressure. Eq. (15) is used to determine the OCR in the laboratory. However, the OCR can also be predicted using an empirical formula obtained from the VST according to the results offered by (Mayne 1991, Worth 1984) as follows

$$OCR = \left[ \frac{C_u / \sigma_v^0}{C_u / \sigma_{v0}'} \right]^{1/m} \quad (16)$$

where  $C_u$  is the undrained strength (kPa),  $\sigma_{v0}'$  is the overburden pressure,  $(S_u / \sigma_{v0}')_{NC}$  is the normalized strength when the OCR is equal to 1.0, and  $m$  is the empirical coefficient, which is equal to 1 according to the results provided by Gao and Chen (2017).

Fig. 20 shows the OCR at different depths. The OCR will decrease as depth increases. However, the data from the conventional oedometer tests are less than that from the VST. The primary reason is that the sampling process is

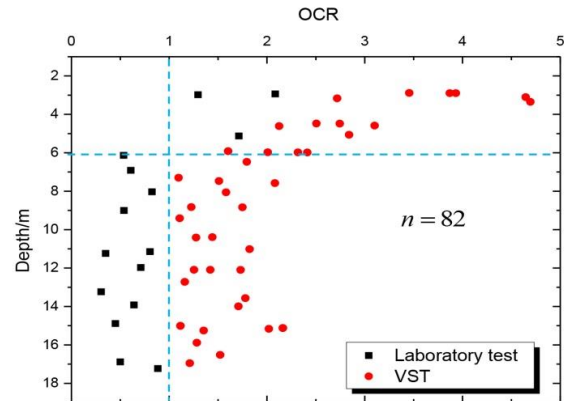


Fig. 20 OCR vs. depth

Table 7 Comparison of the evaluation of consolidation by OCR

Country	City	Soil type	Depth/m	VST		conventional oedometer tests		Gap ratios	Reference
				Average OCR	Consolidation state	Average OCR	Consolidation state		
China	Tianjin	Clay with CH	3-6	2.6(1-5)	Overconsolidation	1.14(1.0-1.43)	Overconsolidation	2.6/1.4=2.28	-
			6-18	1.53(1-2.45)	Overconsolidation	0.6(0.43-0.76)	Underconsolidation	2.55	-
China	Shanghai	Clay with CH	3-12	3.12 (1-6)	Overconsolidation	1.10	Overconsolidation	2.83	Gao and Chen (2017)
			12-25	1.51 (1-2)	Overconsolidation	1.09	Overconsolidation	1.39	Gao and Chen (2017)
China	Zhuhai	Clay with CH	5-10	0.72	Underconsolidation	0.43	Underconsolidation	1.67	He (2010)
			10-27	0.6	Underconsolidation	0.53	Underconsolidation	1.13	He (2010)

bound to have a certain disturbance to the soil samples, and the data from the VST are more reliable than the laboratory in terms of the OCR. The OCR determined using conventional oedometer tests is less than 1 when the depth is greater than 6 m, which demonstrates that Tianjin marine clay is underconsolidated. In contrast, the OCR determined using the VST approaches 1.0, which illustrates that Tianjin marine clay is overconsolidated. The evaluation of the OCR and the consolidation state obtained using the VST and laboratory tests are listed in Table 7 for comparison with other cities in China. The gap ratio is used to characterize the difference between the OCR determined using conventional oedometer tests and the OCR determined using the VST, which reminds engineers to identify the corrected data.

### 3.6 Hydraulic conductivity

According to Terzaghi's one dimensional consolidation theory, the hydraulic conductivity,  $k_v$ , of marine clays can be obtained from the consolidation test using Eq. (17)

$$k_v = C_v m_v \gamma_w \quad (17)$$

where  $m_v$  is the coefficient of volumetric compressibility ( $1/m_v$  is the constrained modulus), and  $\gamma_w$  is the unit weight of water.

Fig. 21 shows that the  $k_v$  of Tianjin marine clay presents a non-linear decreasing trend with an increase in the

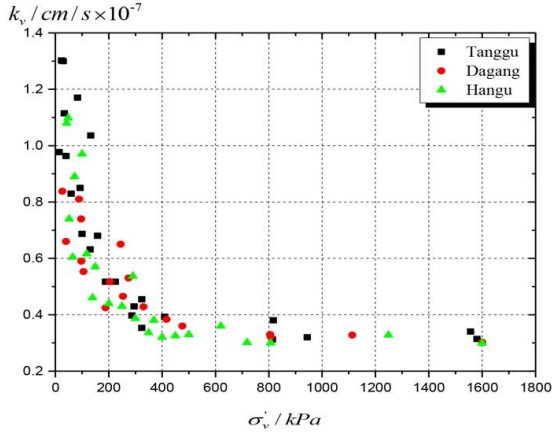
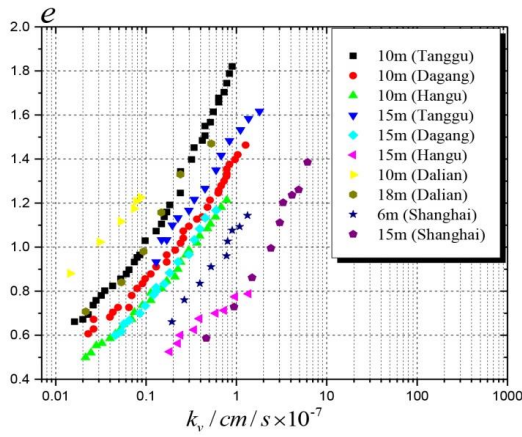

 Fig. 21  $k_v$  versus  $\sigma'_v$ 

 Fig. 22  $e$  versus  $k_v$ 

 Table 8 Hydraulic conductivity change index  $C_{kv}$ 

Type of soil	Depth (m)	Initial void ratio $e_0$	Hydraulic conductivity change index $C_{kv}$	Reference
Tianjin marine clay	10 and 15	1.2 - 1.9	0.50	
Dalian	10 and 18	1.2	0.42	Jiang <i>et al.</i> (2014)
Shanghai	6 and 15	1.35	0.72	Jiang <i>et al.</i> (2014)
Fort Lennox	6.1	2.31	0.931	Tavenas <i>et al.</i> (1983)
St-Hilarie	9.5	1.86	0.745	Tavenas <i>et al.</i> (1983)
Bangkok clay	3	2.31	0.815	Horpibulsuk <i>et al.</i> (2007)
Bangkok clay	7	3.04	1.136	Horpibulsuk <i>et al.</i> (2007)
KGa-1		1.06	0.484	Dolinar (2009)
K-1		1.64	0.543	Dolinar (2009)
Backcebol	4.3	2.28	1.014	Leroueil <i>et al.</i> (1992)
Matagami A	8.8	1.86	0.818	Leroueil <i>et al.</i> (1992)
Matagami B	8.8	1.74	0.808	Leroueil <i>et al.</i> (1992)

consolidation pressure. The  $k_v$  rapidly decreased from a maximum value of  $1.3 \times 10^{-7}$  cm/s to a stable value of approximately  $3.0 \times 10^{-8}$  cm/s at a 400 kPa consolidation pressure.

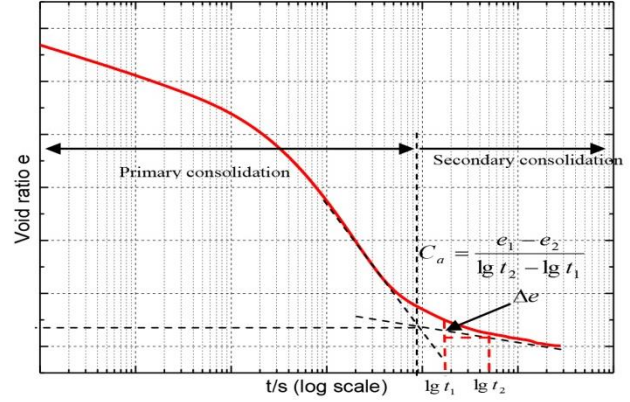

 Fig. 23  $lgt$  versus  $e$ 

Fig. 22 is a plot of the void ratio  $e$  versus  $\log k_v$ , and it shows an overall linear relationship between the void ratio  $e$  and  $\log k_v$  for the Tianjin marine clays in Tanggu, Dagang and Hangu. The clays in Dalian and Shanghai also showed a linear relationship between the void ratio  $e$  and  $\log k_v$  in Fig. 22. Leroueil *et al.* (1992) correlated the void ratio  $e$  and  $\log k_v$ , as expressed in Eq. (18)

$$C_{kv} = \frac{e - e_0}{\lg(k_v / k_{v0})} \quad (18)$$

where  $C_{kv}$  is the hydraulic conductivity change index, which is the slope of the lines in Fig. 22,  $e_0$  is the initial void ratio, and  $k_{v0}$  is the hydraulic conductivity corresponding to the initial void ratio.

The  $C_{kv}$  for Tianjin marine clay is approximately 0.50. Similarly, according to Jiang *et al.* (2014), the values of  $C_{kv}$  for Dalian clay and Shanghai clay are 0.48 and 0.52, respectively. The values of  $C_{kv}$  for the different regions are summarized in Table 8. Table 8 shows that the values of  $C_{kv}$  vary in different regions.

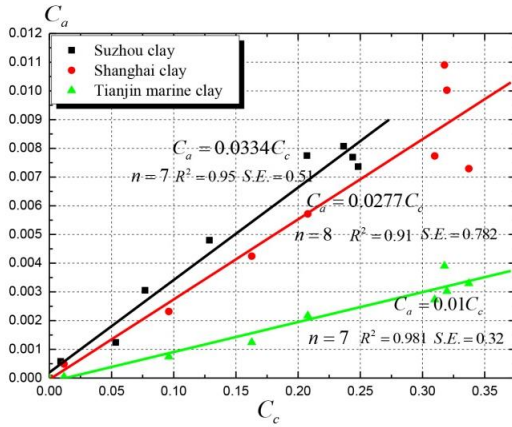
### 3.7 Secondary consolidation

The secondary compression index,  $C_a$ , is an important parameter used to predict the secondary consolidation settlement of Tianjin marine clay. Fig. 23 shows a boundary between the primary and secondary consolidation based on the consolidation curve. The definition of  $C_a$  is expressed by Eq. (19)

$$C_a = \frac{e_1 - e_2}{\lg t_2 - \lg t_1} \quad (19)$$

where  $t_1$  is the time at the end of the primary consolidation completion,  $t_2$  is the time of the secondary consolidation deformation,  $e_1$  is the void ratio at the end of the primary consolidation completion, and  $e_2$  is the void ratio at the secondary consolidation stage.

Fig. 24 is a plot of  $C_a$  versus  $C_c$ . Fig. 24 shows that  $C_a$  approximately linearly increases with  $C_c$  for Tianjin marine clay as well as Suzhou and Shanghai clays. In other words, the ratio of  $C_a/C_c$  remains constant.

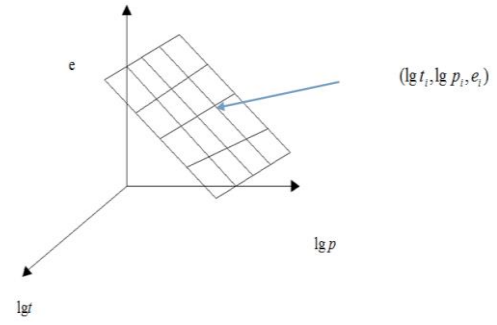
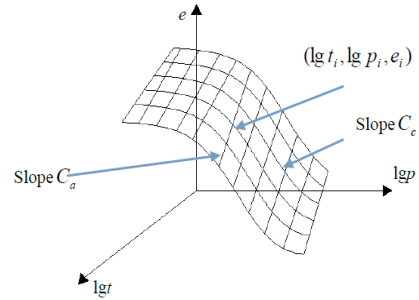
Fig. 24  $C_a$  versus  $C_c$ Table 9  $C_a/C_c$  Values in different regions

Location	Soil type	$C_a/C_c$	Reference
China	Tianjin marine clay	0.0098 - 0.0011	Lei and Xiao (2002)
	Guangzhou clay	0.027 - 0.037	Chen <i>et al.</i> (2005)
	Lianyun bay clay	0.0406 - 0.0468	Zhang <i>et al.</i> (2006)
	Fuzhou clay	0.023 - 0.041	Teng <i>et al.</i> (2008)
	Jiangsu clay	0.042	Miao <i>et al.</i> (2007)
	Ningbo clay	0.056 - 0.0567	Liu <i>et al.</i> (2008)
	Wenzhou clay	0.022 - 0.041	Dan <i>et al.</i> (2009)
European cities	Granular soil including rockfill	$0.02 \pm 0.01$	Mesri and Castro (1987)
	Shale and mudstone	$0.03 \pm 0.01$	Mesri and Castro (1987)
	Inorganic clays and silts	$0.04 \pm 0.01$	Mesri and Castro (1987)
Essen and Mol, Belgium	Organic clays and silts	$0.05 \pm 0.01$	Mesri and Castro (1987)
	Peat and muskeg	$0.075 \pm 0.01$	Mesri and Castro (1987)
	Boom clay	0.02 - 0.04	Deng <i>et al.</i> (2012)
Canada	Berthierville clay	0.045	Mesri and Castro. (1987)
Saudi Arabia	Sabkha Soils	0.037	Al-Shamrani (1998)
Canada	Bearpaw Shale	0.029	Mesri and Castro (1987)

For Tianjin marine clay, the correlation between  $C_a$  and  $C_c$  is expressed by Eq. (20)

$$C_a = 0.001C_c \quad (20)$$

The  $C_a/C_c$  ratios for different regions in China are summarized in Table 9 for comparison purposes. Although the  $C_a/C_c$  ratio of Tianjin marine clay is small compared with that of other regions, the small  $C_a/C_c$  ratio does not mean that the secondary consolidation settlement of Tianjin marine clay is also small. This is because the value of  $C_a$  depends on  $C_a/C_c$  and the value of  $C_c$ . The values of  $C_c$  for Tianjin marine clay are greater than those in other areas, as shown in Fig. 24.

Fig. 25  $e$ - $lg p$ - $lg t$  space planeFig. 26  $e$ - $lg p$ - $lg t$  space curved surface

To explain the different relations between  $C_a$  and  $C_c$ , a three-dimensional space equation,  $e$ - $lg p$ - $lg t$ , was established based on the  $e$ - $lg p$  figure offered by Bjerrum (1973). The direction vector of any lines could be presented by  $\vec{n}_1 = (0, 1, C_c)$  in the  $e$ - $lg p$  figure. Similarly, the direction vector of any lines can be represented by  $\vec{n}_2 = (1, 0, C_a)$  in  $e$ - $lg t$ . Therefore, the normal vector of the space surface can be described as follows

$$\vec{n} = \vec{n}_1 \times \vec{n}_2 = \begin{vmatrix} \vec{i} & \vec{j} & \vec{k} \\ 0 & 1 & C_c \\ 1 & 0 & C_a \end{vmatrix} = C_a \vec{i} + C_c \vec{j} - \vec{k} = (C_a, C_c, -1) \quad (21)$$

A point is selected on  $e$ - $lg p$ - $lg t$ ; hence, the space plane equation is presented below, and the space plane is plotted in Fig. 25.

$$C_a(\lg t - \lg t_i) + C_c(\lg p - \lg p_i) - (e - e_i) = 0 \quad (22)$$

where  $e_i$  is the void ratio and  $p_i$  is the pressure when time is  $t_i$ .

When  $e$  is equal to  $e_0$ , Eq. (22) can be expressed as

$$C_a(\lg t - \lg t_i) + C_c(\lg p - \lg p_i) = (e_0 - e_i) \quad (23)$$

Obviously, the line is projected onto the plane of  $lg t$ - $lg p$ , and  $C_a/C_c$  is constant.

If  $e$ - $lg p$  can satisfy the law of variation given by Crawford, in which the authors consider the change of  $C_a$  with an increase in time. Therefore, a space surface can be drawn as shown in Fig. 26.

Since the compression curve shows a monotonic trend,  $C_a$  varies monotonically with time. When  $e$  is a constant,

the surface is projected into  $\lg t$ - $\lg p$ , which shows a straight line. Moreover, different values of  $e$  lead to different values of  $C_d/C_c$ .

In fact, the different values of  $C_d/C_c$  are due to the different coefficients of compressibility and initial void ratios in different regions, which demonstrates that  $C_a$  is closely related to the soil condition in the local area.

#### 4. Conclusions

This study evaluated the geotechnical characteristics and consolidation properties of Tianjin marine clay. Several correlations between the advanced geotechnical parameters and the basic soil properties were established. The following conclusions can be drawn:

- Tianjin marine clay exhibits high compressibility. Correlations were observed between the following: the water content,  $w_n$ , and the void ratio,  $e_0$ ; the tip resistance,  $q_c$ , and the constrained modulus,  $E_s$  ( $0.2 \text{ MPa} < q_c < 0.7 \text{ MPa}$ ); the undrained shear strength,  $C_u$ , and the depth,  $H$ ; the compression index,  $C_c$ , and the liquid limit,  $LL$ ;  $C_c$  and  $e_0$ ; and  $C_u/P_c$  and  $PL$ . For Tianjin marine clay, the following correlative expressions were found:  $e_0=0.0298w_n-0.27$ ,  $E_s=3.9704q_c+0.029$ ,  $C_u=-3.53H-9.46$ ,  $C_c=0.0107(LL-13)$ , and  $C_c=0.43 e_0-0.05$ ,  $C_u/P_c=0.029PI-0.145$ .

- The engineering geology properties of Tianjin marine clay were researched using laboratory tests and in situ tests. The data indicate that Tianjin marine clay has high plasticity.

- The  $C_c$  value for the Tianjin marine clay in Tanggu is greater than that of the clays in Dagang and Hangu. The ICL of Tianjin marine clay is the same as the ICL proposed by Burland. All the data obtained from Tanggu, Dagang and Hangu at depths of 7-12 m were close to or greater than the SCL, which indicates that the clays have certain structural characteristics.

- The coefficient of consolidation for the Tianjin marine clay in Tanggu is greater than that of the clays in Dagang and Hangu, which indicates that the Tianjin marine clay in Tanggu has a higher rate of consolidation. Additionally, the Tianjin marine clay in Tanggu has greater structural strength (approximately 24.8 kPa-62.7 kPa) than that in Dagang and Hangu.

- The secondary compression indexes,  $C_a$  and  $C_c$ , have a reasonable linear relationship and a correlation coefficient close to 1. The ratio of  $C_a/C_c$  is approximately 0.01.

#### Acknowledgements

The authors would like to acknowledge financial support from the National Natural Science Foundation of China (NSFC) (Grant Nos. 51578371 and 51378344), the Tianjin Research Program of Application Foundation and Advanced Technology (Grant No. 14JCYBJC21700) and the Beijing-Tianjin-Hebei Special Projects of Cooperation (Grant No. 16JCJDJC40000).

#### References

Al-Shamrani, M.A. (1998), "Application of the  $C_a/C_c$ , concept to

- secondary compression of sabkha soils", *Can. Geotech. J.*, **35**(35), 15-26.
- Arulrajah, A. and Bo, M.W. (2008), "Characteristics of Singapore marine clay at Changi", *Geotech. Geol. Eng.*, **26**(4), 431-441.
- Bjerrum, L. (1973), "Problems of soil mechanics and construction of soft clays and structurally unstable soils", *Proceedings of the International Conference on Soil Mechanics and Foundation Engineering*, Moscow, Russia, August.
- Brand, E.W. and Brenner, R.P. (1981), *Soft Clay Engineering*, Elsevier, New York, U.S.A.
- Burland, J.B. (1990), "On the compressibility and shear strength of natural clays", *Géotechnique*, **40**(3), 329-378.
- Cai, G., Liu, S., Tong, L. and Du, G. (2007), "Study on consolidation and permeability properties of Lianyungang marine clay based on piezocone penetration test", *Chin. J. Rock Mech. Eng.*, **26**(4), 846-852.
- Cassagrande, A. (1932), "Research on the Atterberg limits of soils", *Public Roads*, **13**(8), 121-136.
- Chen, B., Xu, Q. and Sun, D. (2014), "An elastoplastic model for structured clays", *Geomech. Eng.*, **7**(2), 213-231.
- Chen, X., Zhu, H., Zhang, Z. and Zhang, B. (2005), "Experimental study on time-dependent deformation of soft soil", *Chin. J. Rock Mech. Eng.*, **24**(12), 2142-2148.
- Chung, S.G., Giao, P.H., Kim, G.J. and Leroueil, S. (2002), "Geotechnical properties of Pusan clays", *Can. Geotech. J.*, **39**(5), 1050-1060.
- Dan, H. (2009), "Time dependent behavior of natural soft clays", Ph.D. Dissertation, Zhejiang University, Hangzhou, China.
- Das, B.M. and Sobhan, K. (2013), *Principles of Geotechnical Engineering*, Cengage Learning.
- Deng, Y.F., Cui, Y.J., Tang, A.M., Li, X.L. and Sillen, X. (2012), "An experimental study on the secondary deformation of Boom clay", *Appl. Clay Sci.*, **59**, 19-25.
- Dolinar, B. (2009), "Predicting the hydraulic conductivity of saturated clays using plasticity-value correlations", *Appl. Clay Sci.*, **45**(1-2), 90-94.
- Du, D.J., Yang, A.W., Liu, J., Liu, H.P., Zhao, R.B. and Zhao, J.J. (2010), *New Dredger Fillings in Binhai District of Tianjin*, China Science Press, Beijing, China.
- Du, Y.J., Liu, S.Y. and Hayashi, S. (2008), "Experimental study on the deterioration and natural remediation of the Ariake Sea tidal mud caused by the sea laver treatment acid practice and the upward seepage of pore water liquid", *Environ. Geol.*, **55**(4), 889-900.
- Ebrahimiyan, B., Movahed, V. and Yousefnia Pasha, A.Y. (2012), "Evaluation of undrained shear strength of marine clay using cone penetration resistance at South Pars field in Iran", *Ocean Eng.*, **54**, 182-195.
- Gao, Y.B. and Chen, Z.Q. (2017), "Analysis of the OCR of soft clay in coastal areas based on field vane strength", *Chin. J. Rock Mech. Eng.*
- Hong, Z. and Tsuchida, T. (1999), "On compression characteristics of Ariake clays", *Can. Geotech. J.*, **36**(5), 807-814.
- Hong, Z.S., Liu, Z.F., Guo, H.L. and Liu, S.Y. (2004), "Relationship between void index and normalized water content for natural sedimentary Ariake clays", *Rock Soil Mech.*, **25**(11), 1698-1701.
- Horpibulsuk, S., Shibuya, S., Fuenkajorn, K. and Katkan, W. (2007), "Assessment of engineering properties of Bangkok clay", *Can. Geotech. J.*, **44**(2), 173-187.
- Hui, H.E. (2010), "Analysis of consolidation historic characteristics of deep soft soil Embankment of Jiangmen-Zhuhai Highway", *J. Railway Eng. Soc.*, **6**, 12.
- Jiang, M.J., Liu, J.D. and Yin, Z.Y. (2014), "Consolidation and creep behaviors of two typical marine clays in China", *Chin. Ocean Eng.*, **28**(5), 629-644.
- Lei, H. and Xiao, S. (2002), "Study on secondary consolidation

- deformation characteristics of soft soil in Tianjin”, *Chin. J. Eng. Geol.*, **10**(4), 385-389.
- Lei, H., Li, B., Qiu, W., Lu, H. and Ren, Q. (2015), “Secondary consolidation characteristics of soft clay foundation of dredger fill site”, *Rock Soil Mech.*, **36**(S1), 120-124.
- Leroueil, S., Leart, P., Hight, D.W. and Powell, J.J.M. (1992), “Hydraulic conductivity of a recent estuarine silty clay at Bothkennar”, *Geotechnique*, **42**(2), 275-288.
- Liu, Y. (2008), “Study on engineering property and application of constitutive model for Ningbo soft clay”, Ph.D. Dissertation, Zhejiang University, Hangzhou, China.
- Ma, J. (2014), “Analysis on consolidation of marine soft soil in Tianjin region”, *Subgrade Eng.*, **5**, 153-157.
- Mayne, P.W. (1991), “Determination of OCR in clays by piezocone tests using cavity expansion and critical state concepts”, *Soils Found.*, **31**(2), 65-76.
- Mayne, P.W., Christopher, B.R. and DeJong, J. (2001), *Manual on Subsurface Investigations, National Highway Institute Publication. FHWA NHI-01-031*, Federal Highway Administration, Washington, D.C., U.S.A.
- Mesri, G. and Castro, A. (1987), “ $C_d/C_c$  concept and  $K_0$  during secondary compression”, *J. Geotech. Eng.* **113**(3), 230-247.
- Mesri, G. and Funk, J.R. (2015), “Settlement of the Kansai International Airport islands”, *J. Geotech. Geoenviron. Eng.*, **141**(2), 04014102.
- Miao, L., Zhang, J. and Chen, Y. (2007), “Study on compressibility of Jiangsu marine clay”, *Chin. J. Geotech. Eng.*, **29**(11), 1711-1714.
- Ministry of Water Resources of the People’s Republic of China (1999), *Specification of Soil Test (SL237-1990)*, China Communications Press, Beijing, China.
- Park, D.S. (2016), “Rate of softening and sensitivity for weakly cemented sensitive clays”, *Geomech. Eng.*, **10**(6), 827-836.
- Shu, X. (2013), “Study of mechanism and countermeasure on asymmetric settlement of soft soil subgrade”, Ph.D. Dissertation, Tianjin University, Tianjin, China.
- Sun, D., Chen, L., Zhang, J. and Zhou, A. (2015), “Bifurcation analysis of over-consolidated clays in different stress paths and drainage conditions”, *Geomech. Eng.*, **9**(5), 669-685.
- Tanaka, H., Locat, J., Shibuya, S., Soon, T.T. and Shiwakoti, D.R. (2001), “Characterization of Singapore, Bangkok, and Ariake clays”, *Can. Geotech. J.*, **38**(2), 378-400.
- Tavenas, F., Jean, P., Leblond, P. and Leroueil, S. (1983), “The permeability of natural soft clays. Part II: Permeability characteristics”, *Can. Geotech. J.*, **20**(4), 645-660.
- Teng, J. and Xiong, C. (2008), “Study of rheology based on soft soil structure”, *J. Changsha Univ.*, **5**, 50-53.
- Terzaghi, K. (1925), “Principles of soil mechanics, IV-settlement and consolidation of clay”, *Eng. News Rec.*, **95**(3), 874-878.
- Tianjin Construction Management Committee (2009), *Technical Specification for Division of Subsoil Sequence in Tianjin (DB/T29-191-2009)*, Communications Press, Beijing, China.
- Wang, C., Yan, S. and Zhang, R. (2007), “Determination of the parameters of visco-elastic-plasticity model for creep of soft clay”, *Rock Soil Mech.*, **28**, 220-224.
- Wang, N. and Wei, R. (1994), “Comparative analysis of sampling quantity for coastal soft clay”, *Chin. J. Eng. Geol.*, **2**(2), 66-75.
- Wang, X. (2014), “Research of accelerated creep properties and microscopic mechanism on soft clay”, M.Sc. Thesis, Tianjin University, Tianjin, China.
- Wei, D. and Hu, Z. (1980), “Experimental study of preconsolidation on pressure and compressibility parameters of Shanghai subsoil”, *Chin. J. Geotech. Eng.*, **2**(4), 13-22.
- Wei, S., Zheng, G. and Liu, C. (2010), “Experimental studies on unloading deformation properties of soft clay in Binhai New Area”, *Hydrogeol. Eng. Geol.*, **37**(5), 77-82.
- Wroth, C.P. (1984), “The interpretation of in situ soil tests”, *Geotechnique*, **34**(4), 449-489.
- Wu, C.J., Ye, G.L., Zhang, L.L., Bishop, D. and Wang, J.H. (2015), “Depositional environment and geotechnical properties of Shanghai clay: A comparison with Ariake and Bangkok clays”, *Bull. Eng. Geol. Environ.*, **74**(3), 717-732.
- Wu, Q. (2015), “Research on influence of bond water on secondary consolidation and long-term strength of soft clay”, Ph.D. Dissertation, Jilin University, Changchun, China.
- Xia, X.F., Xie, G.Y., Shi, X.B. and Xu, L. (2008), “Detection method of deviated group data based on confident interval”, *Comput. Eng.*, **34**(21), 12-14.
- Yang, A. (2011), “Study on rheologic characteristics and its constitutive model of structured soft dredger fill”, Ph.D. Dissertation, Tianjin University, Tianjin, China.
- Yang, A., Yan, S., Du, D., Zhao, R. and Liu, J. (2010), “Experimental study of alkaline environment effects on the strength of cement soil of Tianjin marine soft soil”, *Rock Soil Mech.*, **31**(9), 2930-2934.
- Yang, T.L. and Gong, S.L. (2010), “Microscopic analysis of the engineering geological behavior of soft clay in Shanghai, China”, *Bull. Eng. Geol. Environ.*, **69**(4), 607-615.
- Yin, J., Hong, Z. and Gao, Y. (2009), “Yielding characteristics of natural soft Lianyungang clay”, *J. Southeast Univ. Nat. Sci. Ed.*, **39**(5), 1059-1064.
- Yoon, G.L., Kim, B.T. and Sang, S.J. (2011), “Empirical correlations of compression index for marine clay from regression analysis”, *Can. Geotech. J.*, **41**(6), 1213-1221.
- Zhang, H. (2010), “Research on mechanical analysis for Beijing-Tianjing-Tangshan expressway based on old road with three dimensional horizontal crack”, M.Sc. Thesis, Changan University, Xi’an, China.
- Zhang, J., Huang, X. and Miao, L. (2006), “Research on engineering properties of Lianyungang soft clay”, *Chin. J. Highway Transport. Res. Dev.*, **23**(2), 10-14.
- Zheng, G., Zhang, X., Diao, Y. and Lei, H. (2016), “Experimental study on the performance of compensation grouting in structured soil”, *Geomech. Eng.*, **10**(3), 335-355.

CC